5810 *Biochemistry* **2010,** *49,* 5810–5816
DOI: 10.1021/bi1004969

BIOCHEMISTRY
including biophysical chemistry & molecular biology
Article

Long-Range Electron Transfer Reactions between Hemes of MauG and Different Forms of Tryptophan Tryptophylquinone of Methylamine Dehydrogenase[†]

Sooim Shin, Nafez Abu Tarboush, and Victor L. Davidson*

Department of Biochemistry, The University of Mississippi Medical Center, Jackson, Mississippi 39216

Received April 2, 2010; Revised Manuscript Received May 17, 2010

ABSTRACT: The diheme enzyme MauG catalyzes the post-translational modification of a precursor protein of methylamine dehydrogenase (preMADH) to complete the biosynthesis of its protein-derived tryptophan tryptophylquinone (TTQ) cofactor. This six-electron oxidation of preMADH requires long-range electron transfer (ET) as the structure of the MauG−preMADH complex reveals that the shortest distance between the modified residues of preMADH and the nearest heme of MauG is 14.0 Å [Jensen, L. M. R., Sanishvili, R., Davidson, V. L., and Wilmot, C. M. (2010) *Science 327*, 1392−1394]. The kinetics of two ET reactions between MADH and MauG have been analyzed. Interprotein ET from quinol MADH to the high-valent bis-Fe(IV) form of MauG exhibits a K_d of 11.2 μM and a rate constant of 20 s^{-1}. ET from diferrous MauG to oxidized TTQ of MADH exhibits a K_d of 10.1 μM and a rate constant of 0.07 s^{-1}. These similar K_d values are much greater than that for the MauG−preMADH complex, indicating that the extent of TTQ maturity rather than its redox state influences complex formation. The difference in rate constants is consistent with a larger driving force for the faster reaction. Analysis of the structure of the MauG−preMADH complex in the context of ET theory and these results suggests that direct electron tunneling between the residues that form TTQ and the five-coordinate oxygen-binding heme is not possible, and that ET requires electron hopping via the six-coordinate heme.

Methylamine dehydrogenase (MADH)[1] is a 119 kDa hetero-tetrameric $\alpha_2\beta_2$ protein (*1*, *2*), with each β subunit possessing a tryptophan tryptophylquinone (TTQ) (*3*) protein-derived cofactor (*4*). TTQ is formed by post-translational modification of two tryptophan residues of the polypeptide chain. For TTQ biosynthesis, two atoms of oxygen are incorporated into the indole ring of βTrp57, and a covalent bond is formed between the indole rings of βTrp57 and βTrp108. TTQ biosynthesis requires the action of MauG (*5*) which is a 42.3 kDa enzyme containing two *c*-type hemes (*6*). MauG exhibits homology to diheme cytochrome *c* peroxidase (*7*, *8*) but displays significant differences in catalytic and redox behavior (*9*, *10*). Inactivation of *mauG*, a gene in the methylamine utilization (*mau*) gene cluster (*11*), leads to the accumulation of a biosynthetic precursor protein (preMADH) in which βTrp57 is monohydroxylated at the C7 position, and the covalent cross-link between βTrp57 and βTrp108 is absent (*12*, *13*). Incubation of preMADH in vitro with MauG in the presence of either O_2 with an electron donor or H_2O_2 as oxidizing equivalents ([O]) results in completion of TTQ biosynthesis and active MADH (*5*, *9*).

The TTQ biosynthetic reactions proceed via a relatively stable high-valent bis-Fe(IV) intermediate with one heme as Fe(IV)=O and the other as Fe(IV) with two axial ligands from the protein (*14*). The sole axial ligand for the ferryl heme is His35, and the axial ligands for the other heme are His205 and Tyr294 (*15*). While the order is not known, the overall process of MauG-dependent TTQ biosynthesis requires three sequential two-electron oxidations to catalyze the second hydroxylation of βTrp57, formation of the cross-link between βTrp57 and βTrp108, and the oxidation to the quinone state.

As TTQ is a two-electron redox cofactor, it may be present in MADH in three different redox states. The fully oxidized quinone exhibits a broad absorbance centered at 440 nm; the one-electron-reduced semiquinone exhibits an absorption maximum at 428 nm, and the fully reduced quinol exhibits an absorption maximum at 330 nm (*16*). The quinol was postulated to be an intermediate in TTQ biosynthesis from preMADH because a transient intermediate with a λ_{max} at 330 nm was observed early in the steady-state TTQ biosynthesis reaction using preMADH as a substrate (*9*). To test this hypothesis, the quinol was formed in vitro by reduction of MADH with dithionite and then tested as a substrate for MauG. Quinol MADH was not oxidized by H_2O_2 alone, but in the presence of MauG, H_2O_2-dependent oxidation of the quinol to TTQ was observed, suggesting that this might be the final step in TTQ biosynthesis in vivo. As such, the steady-state kinetic reaction of MauG-dependent TTQ formation from quinol MADH was studied and compared to the steady-state reaction with preMADH as the substrate for TTQ biosynthesis (Scheme 1).

The kinetic mechanism of initial two-electron oxidation of preMADH by bis-Fe(IV) MauG was previously characterized (*17*).

[†]This work was supported by National Institutes of Health Grant GM-41574.

*To whom correspondence should be addressed: Department of Biochemistry, University of Mississippi Medical Center, 2500 N. State St., Jackson, MS 39216-4505. Telephone: (601) 984-1516. Fax: (601) 984-1501. E-mail: vdavidson@umc.edu.

[1]Abbreviations: MADH, methylamine dehydrogenase; TTQ, tryptophan tryptophylquinone; preMADH, biosynthetic precursor protein of MADH with incompletely synthesized TTQ; ET, electron transfer; bis-Fe(IV) MauG, redox state of MauG with one heme as Fe(IV)=O and the other as Fe(IV); [O], oxidizing equivalents; E_m, oxidation−reduction midpoint potential; H_{AB}, electronic coupling; λ, reorganization energy; ρ, atomic packing density; PDB, Protein Data Bank.

 Published on Web 06/11/2010

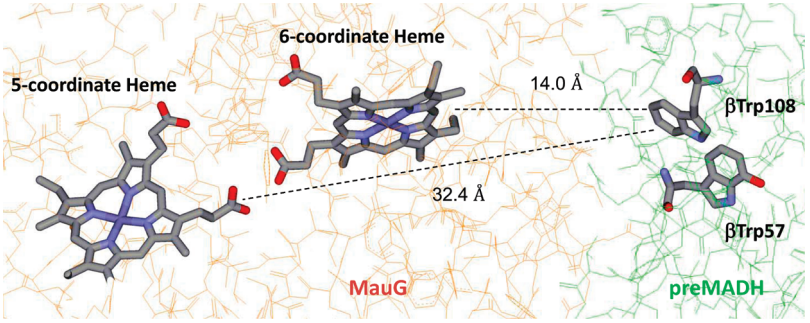

FIGURE 1: Orientation of hemes and residues of interest within the MauG−preMADH complex. A portion of the crystal structure (PDB entry 3L4M) (*15*) is shown. Residues Trp57 and Trp108 of the β subunit of MADH, which are post-translationally modified to form TTQ, and the two hemes of MauG are displayed as sticks. Other residues of MADH (green) and MauG (orange) are displayed as lines. The shortest distances between residue βTrp108 and any portion of each heme, including side chains, are indicated.

Scheme 1

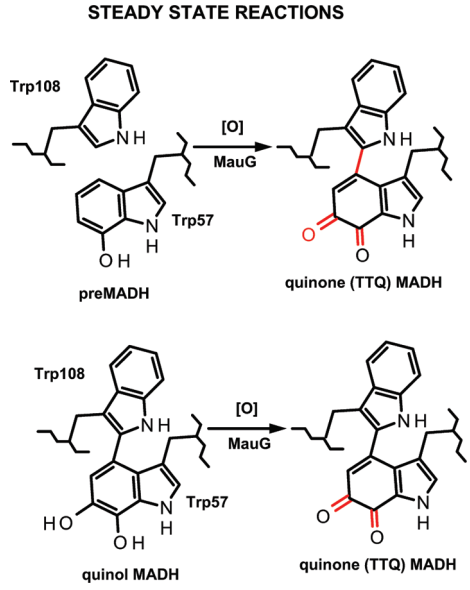

The reaction exhibited a random kinetic mechanism, in which the order of addition of [O] and preMADH did not matter. Such a random mechanism is in contrast to that typically seen for heme-dependent oxygenases but very reasonable given the recently determined crystal structure of the MauG−preMADH complex (*15*). This structure revealed that the residues that are modified to form TTQ do not make direct contact with either heme of MauG (Figure 1). The shortest distance between βTrp108 of preMADH and the oxygen-binding five-coordinate heme is 32.4 Å, and the shortest distance to the six-coordinate heme is 14.0 Å. Given the complexity of the overall biosynthetic reaction and the highly unusual structure of the enzyme−substrate protein complex, it is of particular interest to characterize and compare the kinetics of the different redox reactions that occur between the hemes of MauG and different redox states of TTQ and biosynthetic intermediates of TTQ within the protein complex.

Single-turnover kinetic techniques were used to examine and compare multiple reactions of MauG with MADH and preMADH (Scheme 2). The rate and binding constants for the two-electron oxidation of quinol MADH by bis-Fe(IV) MauG were shown to be quite different from those for the first two-electron oxidation of preMADH by bis-Fe(IV) MauG. Both of these biosynthetic reactions require generation of the bis-Fe(IV) redox state of MauG for their respective electron transfer (ET) to be thermodynamically favorable. Comparison of the oxidation−reduction midpoint potential (E_m) values of the quinone MADH/quinol MADH and bis-Fe(III)/bis-Fe(II) redox couples reveals that in the mature proteins, in the absence of the Fe(IV) state, the thermodynamically favorable reaction is that from the reduced diferrous MauG to the oxidized TTQ in MADH. This is the reverse direction for ET relative to the biosynthetic reactions. This redox reaction was also studied and compared with the two biosynthetic two-electron oxidation reactions. The results reveal the relative importance of the redox states of MauG and MADH, and the extent of TTQ biosynthesis, with regard to the affinity of the proteins for each other. Analysis of the structure of the MauG−preMADH complex in the context of ET theory and these experimental results also provides insight into possible mechanisms of the long-range ET which is required for the biosynthetic and redox reactions that occur within the protein complex.

EXPERIMENTAL PROCEDURES

Protein Purification. MauG (*6*) and MADH (*18*) were purified from *Paracoccus denitrificans* as described previously, and protein concentrations were calculated using the following extinction coefficients for diferric MauG (ε_{406} = 309000 M^{-1} cm^{-1}), quinone MADH (ε_{440} = 26200 M^{-1} cm^{-1}), and quinol MADH (ε_{330} = 56400 M^{-1} cm^{-1}).

Steady-State Kinetic Experiments. Steady-state kinetic studies of MauG-dependent oxidation of quinol MADH were performed using a previously described spectrophotometric assay (*9*). MauG (0.07 μM) was mixed with varied concentrations of quinol MADH in 0.01 M potassium phosphate buffer at pH 7.5 and 25 °C. Reactions were initiated by addition of 1 mM H_2O_2. The reaction was monitored by the rate of appearance of the oxidized MADH at 440 nm. Data were fit to eq 1

$$v/[E] = k_{cat}[S]/([S] + K_m) \quad (1)$$

where S is quinol MADH, E is MauG, v is the initial reaction velocity, k_{cat} is the turnover number, and K_m is the Michaelis constant.

Single-Turnover Kinetic Experiments. Transient kinetic experiments of the reactions of bis-Fe(IV) MauG with quinol MADH were performed using an Online Instrument Systems (OLIS, Bogart, GA) RSM stopped-flow spectrophotometer. Kinetic data collected in the rapid-scanning mode were reduced by factor analysis using the singular-value decomposition algorithm and then globally fit using the fitting routines of OLIS Global Fit. All reactions were performed in 0.01 M potassium phosphate buffer at pH 7.5 and 25 °C. Prior to mixing, one

Scheme 2

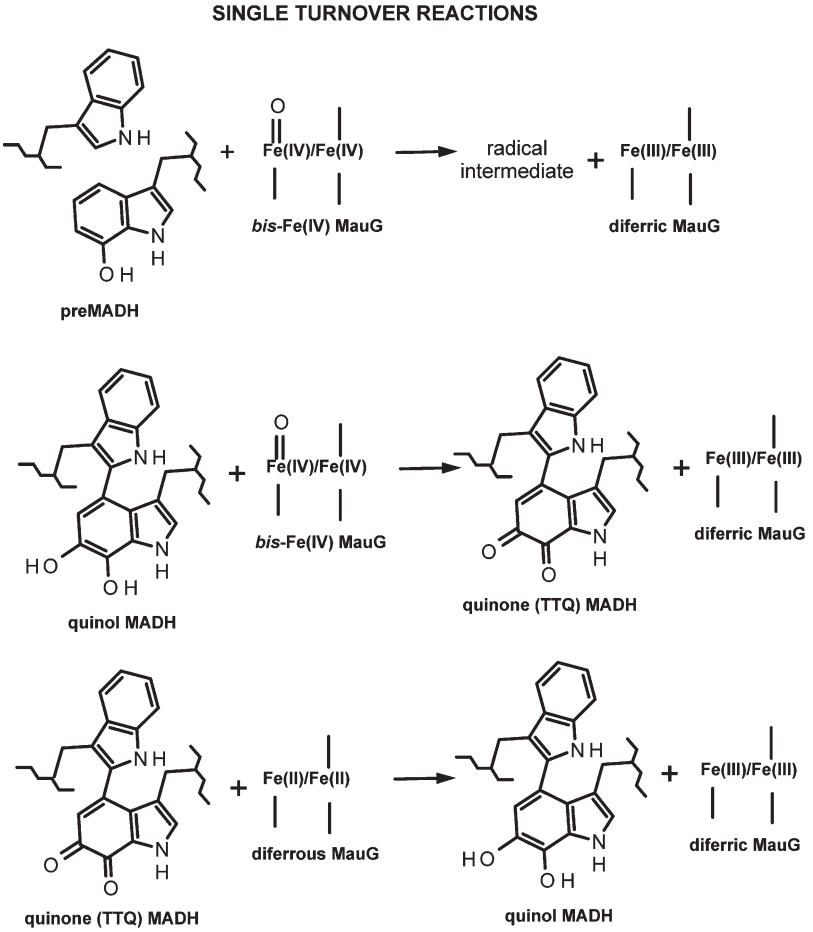

syringe contained a fixed concentration of 2 μM bis-Fe(IV) MauG that was generated by stoichiometric addition of H_2O_2 and the other contained varied concentrations of quinol MADH. Both the bis-Fe(IV) state of MauG (*14*) and the quinol form of MADH (*19*) are sufficiently stable that negligible amounts of either diferric MauG or quinone MADH are present. Reactions were monitored between 366 and 446 nm to observe the conversion of bis-Fe(IV) MauG to diferric MauG. The observed rates were best fit to a single exponential, and the limiting first-order rate constant (k_3) for the reaction of MauG with reduced MADH was determined from the concentration dependence of the observed rate using eqs 2 and

$$E + S \underset{}{\overset{K_d}{\rightleftharpoons}} ES \underset{k_4}{\overset{k_3}{\rightleftharpoons}} E'P \quad (2)$$

$$k_{obs} = k_3[S]/([S] + K_d) + k_4 \quad (3)$$

where [S] is the concentration of the quinol MADH, E is bis-Fe(IV) MauG, E′ is diferric MauG, and P is quinone MADH.

To determine whether the kinetic mechanism of the reactions of MauG with H_2O_2 and quinol MADH is random or ordered, experiments were repeated using a different configuration in which one syringe contained diferric MauG with quinol MADH in complex and the other contained H_2O_2, as described previously for the reaction of preMADH with MauG (*17*).

Transient kinetic experiments aimed at elucidating the reactions of diferrous MauG with quinone MADH were performed using a Shimadzu Multispec-1501 spectrophotometer. Reaction mixtures contained a fixed concentration of diferrous MauG (1.25 μM) that was generated by stoichiometric addition of dithionite, and varied concentrations of quinone MADH. The reaction was performed under anaerobic conditions to ensure that MauG remained reduced prior to and during reaction with MADH. The reaction was monitored by the decrease in absorbance at 550 nm which corresponds to the conversion of diferrous MauG to diferric MauG (*6*). Data were analyzed as described above using eqs 2 and 3.

Electron Transfer Rate Predictions. The HARLEM computer program (*20*) was used to calculate atomic packing density (ρ), relative values of electronic coupling (H_{AB}), and maximum predicted ET rates from the crystal structure of the MauG−preMADH complex (PDB entry 3L4M) using the direct distance approach of Dutton and co-workers (*21*). This information was interpreted in the context of ET theory (eqs 4 and 5) (*22*). The other terms in these equations are the reorganization energy (λ), Planck's constant (h), the temperature (T), the gas constant (R), and the characteristic frequency of nuclei ($k_0 = 10^{13}$ s^{-1}) which is the maximum ET rate when donor and acceptor are in van der Waals contact and $\lambda = -\Delta G°$. The parameter β is used to quantitate the nature of the intervening medium with respect to its efficiency to mediate ET. The donor−acceptor distance is r, and r_0 is the close contact distance (3 Å).

$$k_{ET} = [4\pi^2 H_{AB}{}^2/h(4\pi\lambda RT)^{0.5}] \exp[-(\Delta G° + \lambda)^2/4\lambda RT] \quad (4)$$

$$k_{ET} = k_0 \exp[-\beta(r - r_0)] \exp[-(\Delta G° + \lambda)^2/4\lambda RT] \quad (5)$$

RESULTS

Steady-State Kinetic Analysis of MauG-Dependent TTQ Biosynthesis with Quinol MADH as the Substrate. Previous

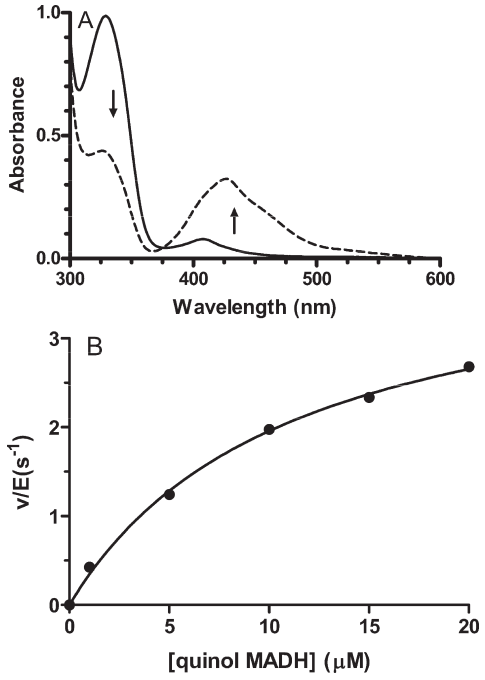

FIGURE 2: Steady-state MauG-depedent TTQ biosynthesis using quinol MADH as a substrate. (A) Spectral changes associated with the conversion of quinol MADH (—) to quinone MADH (---) during the steady-state TTQ biosynthesis reaction. (B) Steady-state kinetic analysis of MauG-dependent oxidation of quinol MADH to quinone MADH by H_2O_2. Each reaction mixture contained 0.07 μM MauG, and the reaction was initiated by addition of 1 mM H_2O_2. The reaction was monitored by following the increase in absorbance at 440 nm. Initial rates were determined in the presence of varying concentrations of quinol MADH. The solid line is the fit of the data to eq 1.

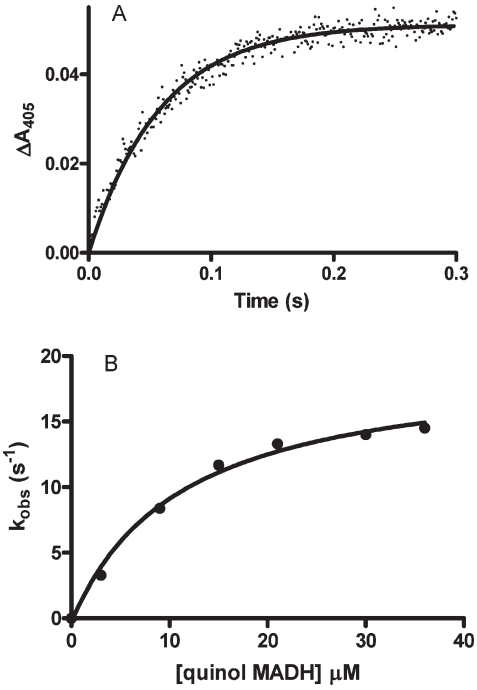

FIGURE 3: Single-turnover kinetics of the reaction of bis-Fe(IV) MauG with quinol MADH. (A) A representative reaction is shown in which prior to the reaction MauG (2 μM) was mixed with a stoichiometric amount of H_2O_2 to generate the bis-Fe(IV) state. The reaction was then initiated by mixing this with quinol MADH (30 μM). The solid line represents the fit of the data to a single-phase exponential rise. The same value of k_{obs} was obtained when the data for the entire range of wavelengths were globally fit. (B) Concentration dependence of the rate of reaction of bis-Fe(IV) MauG with quinol MADH. The solid line is a fit of the data to eq 3.

studies suggested that the final two-electron oxidation during TTQ biosynthesis from preMADH is the oxidation of the quinol form of the cofactor to the quinone (i.e., TTQ). The steady-state reaction of MauG-dependent TTQ biosynthesis from quinol MADH was studied using the steady-state spectrophotometric assay developed previously for MauG-dependent TTQ biosynthesis from preMADH (*17*). The conversion of substrate (quinol MADH) to product (quinone MADH) is accompanied by a decrease in absorbance at 330 nm concomitant with an increase in absorbance at 440 nm (Figure 2A). These experiments yielded a K_m of 11.1 ± 1.3 μM and a k_{cat} of 4.2 ± 0.1 s^{-1} (Figure 2B). It is noteworthy that this k_{cat} value is 20-fold greater than the k_{cat} value of 0.2 s^{-1} that was previously reported for the steady-state reaction when preMADH was used as the substrate. This indicates that the final oxidation of the quinol to the quinone is not the rate-limiting step for the overall biosynthetic process.

MauG exhibits a high affinity for H_2O_2 which did not allow for determination of a precise K_m value for H_2O_2. The initial rate was independent of H_2O_2 concentration down to 5 μM. The amount of product formed in the steady-state reaction cannot exceed the amount of H_2O_2, and at lower concentrations, it became difficult to accurately measure initial velocities because of the small amount of product formed. An affinity for H_2O_2 in the low micromolar range is consistent with results of previous stopped-flow kinetic studies that showed that the rate of formation of bis-Fe(IV) MauG after mixing with H_2O_2 was too fast to measure unless substoichiometric concentrations of H_2O_2 were used (*17*). Such a high affinity is not unprecedented as the diheme cytochrome *c* peroxidase from *Pseudomonas stutzeri* was shown to exhibit half-maximal turnover at 1.8 μM H_2O_2 (*23*).

Analysis of the Reaction of bis-Fe(IV) MauG with Quinol MADH by Single-Turnover Kinetics. The reaction of bis-Fe(IV) MauG with quinol MADH was examined using the protocol previously developed to directly monitor the reaction of bis-Fe(IV) MauG with preMADH (*17*). The reaction rate was determined from the spectral changes which are associated with the conversion of the bis-Fe(IV) MauG species back to the diferric state (Figure 3A) (*17*). The dependence of the observed rate of the reaction on quinol MADH concentration is shown in Figure 3B. It exhibits saturation behavior, and the fit of the data to eq 3 yields a limiting first-order rate constant (k_3) for the reaction of 20.0 ± 1.3 s^{-1}. This value is 10^5-fold greater than the spontaneous rate of decay of bis-Fe(IV) MauG of 2 × 10^{-4} s^{-1} (*17*) and 25-fold greater than the limiting first-order constant of 0.8 s^{-1} for the initial two-electron oxidation reaction of bis-Fe(IV) MauG with preMADH (Table 1) (*17*). The k_3 value is also 5-fold greater than the steady-state k_{cat} for MauG-dependent TTQ biosynthesis from quinol MADH, indicating that some reaction step other than ET, perhaps product release, is rate-limiting for the steady-state biosynthetic reaction when quinol MADH is the substrate. Interestingly, the K_d value of 11.2 ± 2.3 μM for the formation of the bis-Fe(IV) MauG−quinol MADH complex is much greater than the previously determined K_d value of ≤1.5 μM for the bis-Fe(IV) MauG−preMADH complex (Table 1).

For many heme-dependent oxygenases, including cytochrome P450-dependent monooxygenases (*24*, *25*), the enzyme is not reactive toward oxygen in the absence of substrate. It was previously established that this is not true for the first two-electron oxidation reaction of MauG-dependent TTQ biosynthesis, in

Table 1: Single-Turnover Kinetic Parameters for Reactions between Different Forms of MauG and MADH and Its Precursor Proteins

reaction	K_d (μM)	k_3 (s^{-1})
preMADH + bis-Fe(IV) MauG[a]	≤ 1.5	0.8 ± 0.1
quinol MADH + bis-Fe(IV) MauG	11.2 ± 2.3	20 ± 1.3
diferrous MauG + quinone MADH	10.1 ± 1.6	0.07 ± 0.01

[a]Taken from ref *17*.

which the order of addition of [O] and substrate is random (*17*). As such, the effect of the order of addition of quinol MADH and H_2O_2 to MauG was examined. Similarly, the presence of quinol MADH did not influence the kinetics of the reaction of MauG with H_2O_2, and the reaction rate of preformed bis-Fe(IV) MauG with quinol MADH was the same as when bis-Fe(IV) MauG was generated within the preformed protein complex (data not shown). Thus, the kinetic mechanism for this putative final two-electron oxidation step of TTQ biosynthesis also follows a random kinetic mechanism.

Reaction of bis-Fe(II) MauG with Quinone MADH. The biosynthetic reactions catalyzed by MauG and discussed above each require formation of the bis-Fe(IV) state to oxidize the respective protein substrates (see Scheme 2). The E_m value of the bis-Fe(IV)/bis-Fe(III) redox couple is unknown, but it is presumably very positive, allowing the biosynthetic oxidation reactions to be thermodynamically favorable. The E_m values for the bis-Fe(III)/bis-Fe(II) redox couple and the quinone/quinol MADH redox couple are known. Each is a two-electron oxidation−reduction reaction. For MauG, the E_m values for the first and second electron reductions are −159 and −244 mV, respectively (*10*). For MADH, the E_m values for the quinone/semiquinone and semiquinone/quinol couples are +14 and +190 mV, respectively (*26*). Thus, in the absence of the high-valent bis-Fe(IV) state, the thermodynamically favored direction of ET is from diferrous MauG to quinone MADH, the opposite direction versus that for the biosynthetic reactions. This "reverse" reaction from diferrous MauG to oxidized MADH was studied under single-turnover conditions (Figure 4). The reaction exhibited saturation behavior, and analysis of the data yielded a k_3 of 0.07 ± 0.01 s^{-1} and a K_d of 10.1 ± 1.6 μM.

Calculations of ET Efficiency through the MauG−preMADH Complex. The maximum possible ET rates under activationless conditions (i.e., $-\Delta G^\circ = \lambda$) between the residues that are modified to form TTQ, and either heme of MauG, were predicted from the structure of the MauG−preMADH complex using HARLEM and the direct distance approach of Dutton and co-workers (*21*) (Table 2). For this analysis, the shortest distance between residue βTrp108 of MADH and the five-coordinate oxygen-binding heme is 32.4 Å, and given the calculated β and H_{AB}, the maximum possible ET rate is predicted to be $\sim 10^{-9}$ s^{-1}. For ET between residue βTrp108 of MADH and the six-coordinate heme of MauG, the shortest distance is 14.0 Å, and the maximum possible predicted ET rate is $\sim 10^4$ s^{-1}.

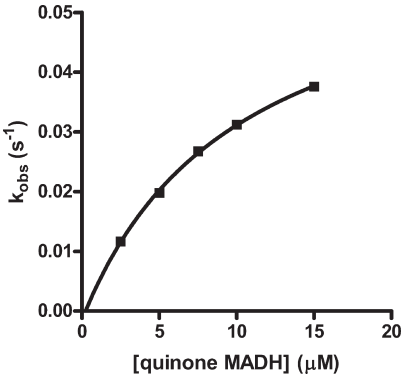

FIGURE 4: Single-turnover kinetics of the reaction of diferrous MauG with quinone MADH. Reaction mixtures contained a fixed concentration of diferrous MauG (1.25 μM) and varied concentrations of quinone MADH. The data for the concentration dependence of the rate are fit to eq 3.

Table 2: Calculated Electron Transfer Properties from the Structure of the MauG−preMADH Complex[a]

	βTrp108 to five-coordinate heme	βTrp108 to six-coordinate heme
distance (Å)	32.4	14.0
atom packing density (ρ)[b]	0.63	0.60
average decay exponential (β)[c] ($Å^{-1}$)	1.61	1.65
relative H_{AB} value[d]	5.24×10^{-12}	1.07×10^{-5}
maximum k_{ET} (s^{-1})[e]	2.7×10^{-9}	1.1×10^4

[a]Calculations using HARLEM (*20*) (http//www.kurnikov.org/harlem_manual/html/index.html) and the structure of the preMADH−MauG complex (PDB entry 3L4M). Waters were not included in the calculation. The relevant portion of the structure is displayed in Figure 1. [b]Volume fraction between redox cofactors within the united van der Waals radius of intervening atoms. [c]β is a parameter in the term $e^{-\beta R}$ that represents the exponential falloff of the electronic tunneling rate with distance. [d]H_{AB} is the electronic tunneling coupling matrix element between the donor and acceptor in dimensionless units for relative comparison. [e]The predicted free energy-optimized rate of electron transfer when $\Delta G = -\lambda$.

DISCUSSION

MauG catalyzes the six-electron oxidation of preMADH to yield oxidized MADH with the mature TTQ cofactor. The overall reaction requires three catalytic cycles of two-electron oxidations. The recently reported crystal structure of the MauG−preMADH complex (*15*) revealed an unexpected orientation of the proteins in which there is no direct contact between either heme of MauG and residue βTrp57 or βTrp108 of preMADH. The shortest distance between the modified residues of preMADH and the nearest heme of MauG is 14.0 Å (Figure 1). Despite the lack of direct contact, it was demonstrated that on addition of H_2O_2 to the crystal, TTQ biosynthesis was catalyzed in the crystalline state. This indicated that long-range ET is critical for each of the catalytic cycles of MauG-dependent TTQ biosynthesis. This raises the possibility that long-range ET rather than the chemical reaction step may be rate-determining for one or more of the three oxidation reactions required for TTQ biosynthesis.

The kinetic mechanism of the first two-electron oxidation of preMADH by MauG was previously characterized (*17*). In this study, the MauG-dependent oxidation of quinol MADH has been characterized, as well as the ET reaction from diferrous MauG to oxidized MADH. This allows the comparison of the rates and binding constants for these three different reactions that occur within the MauG−preMADH complex (see Scheme 2).

It is noteworthy that the K_d value for the preMADH−bis-Fe(IV) MauG complex is significantly lower than that for either the quinol MADH−bis-Fe(IV) MauG or quinone MADH−bis-Fe(II) MauG complex and that the K_d values for the latter two are nearly equal (Table 2). This result is consistent with a previous report that preMADH and MauG coelute during size exclusion chromatography whereas mature MADH and MauG do

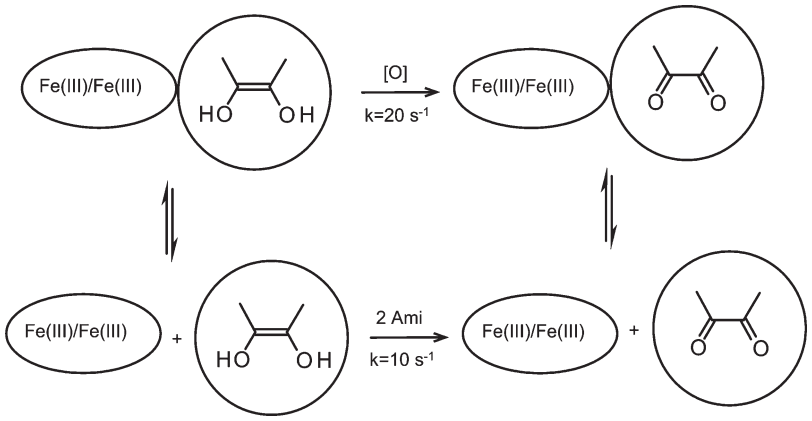

FIGURE 5: Alternative pathway for oxidation of quinol MADH if released from the complex with MauG. Quinol MADH may react with two molecules of its natural electron acceptor, the type 1 copper protein amicyanin (Ami). The rate of that reaction is taken from ref *32*.

not (*27*). In the complexes of quinol MADH with bis-Fe(IV) MauG, and quinone MADH with bis-Fe(II) MauG, MADH and MauG are present in different redox states yet the K_d values are similar. This suggests that neither the redox state of TTQ nor the redox state of the hemes of MauG significantly affects the affinity of MADH and MauG for each other. It is not surprising that quinol MADH dissociates from MauG to the same extent as the final quinone product. Should release of quinol MADH from MauG occur in vivo prior to the final oxidation step, quinol MADH could alternatively be oxidized to the quinone by its natural electron acceptor amicyanin (*28*) (Figure 5). Most significantly, the presence of mature TTQ (either quinol or quinone) versus the incompletely formed TTQ in preMADH does affect the affinity. This is intuitively expected as the product of an enzyme-catalyzed reaction typically has a lower affinity for the enzyme than the substrate. However, this result is surprising given that the crystal structure of the MauG−preMADH complex shows the structure of preMADH to be essentially the same as MADH except for the incomplete formation of TTQ, which is buried within the protein (*15*).

While the ET reaction from diferrous MauG to oxidized MADH is not required for TTQ biosynthesis, the ability to monitor this thermodynamically favorable reaction is a valuable mechanistic tool. In contrast to the biosynthetic oxidation reactions, it does not require formation of the bis-Fe(IV) state. Thus, it is possible to study an ET reaction for which $\Delta G°$ is known within a defined protein structure, independent of the catalytic reactions. Furthermore, in future structure−function studies, comparative analysis of the effects of site-directed mutations on these different redox reactions will allow discrimination of effects of mutations that specifically affect long-range ET from those that affect formation or stabilization of the bis-Fe(IV) state.

The structure of the MauG−preMADH complex revealed that long-range ET is required for catalysis (Table 2 and Figure 1). The 25-fold greater rate of reaction of quinol MADH with bis-Fe(IV) MauG compared to that with preMADH is consistent with the driving force for the redox reaction controlling the reaction rate, rather than some other factor such as a protein conformational change. Calculation of the possible ET rates through the MauG−preMADH complex (Table 2) under activationless conditions (i.e., $-\Delta G° = \lambda$) predicted a maximum possible rate of $\sim 10^{-9}$ s^{-1} for ET from residue βTrp108 of MADH and the five-coordinate oxygen-binding heme. This suggests that direct ET between these points is not a physiologically relevant possibility. For ET between residue βTrp108 of MADH and the six-coordinate heme of MauG, the predicted maximum possible ET rate is $\sim 10^4$ s^{-1}. On this basis, it is clear that electrons which are extracted from preMADH by bis-Fe(IV) MauG must enter the diheme system via the six-coordinate heme rather than the oxygen-binding five-coordinate heme. It is important to note that these ET reactions are not activationless, as assumed in the ET rate predictions, and therefore, the actual ET rate will be less than 10^4 s^{-1}. Further studies are required to attempt to experimentally determine values of λ and H_{AB} for each of these ET reactions for correlation with the structural information. However, the current information indicates that the long-range ET required for these reactions cannot occur via a single long-range tunneling event between TTQ, or residues that are modified to form TTQ, and the five-coordinate heme which binds O_2 and H_2O_2. At the least, the ET requires hopping via the six-coordinate heme.

It has been shown that efficient ET over very long distances through proteins, as well as nucleic acids, may be achieved via a mechanism of hopping rather than via a single direct electron tunneling event (*29*). Such electron hopping mechanisms have been proposed for long-range ET in ribonucleotide reductase (*30*) and DNA photolyase (*31*). In a hopping mechanism, the observed rate will be that of the least efficient hop rather than that of a single tunneling event over the entire distance. Future studies of the effects of mutagenesis of residues at the heme sites which alter the E_m value, as well as residues along predicted ET pathways and at the interface between proteins, should allow a complete description of the long-range ET reactions that are critical for TTQ biosynthesis.

ACKNOWLEDGMENT

We thank Dr. Sheeyong Lee and Yu Tang for helpful discussions and technical assistance.

REFERENCES

1. Davidson, V. L. (2001) Pyrroloquinoline quinone (PQQ) from methanol dehydrogenase and tryptophan tryptophylquinone (TTQ) from methylamine dehydrogenase. *Adv. Protein Chem. 58*, 95–140.
2. Chen, L., Doi, M., Durley, R. C., Chistoserdov, A. Y., Lidstrom, M. E., Davidson, V. L., and Mathews, F. S. (1998) Refined crystal structure of methylamine dehydrogenase from *Paracoccus denitrificans* at 1.75 Å resolution. *J. Mol. Biol. 276*, 131–149.
3. McIntire, W. S., Wemmer, D. E., Chistoserdov, A., and Lidstrom, M. E. (1991) A new cofactor in a prokaryotic enzyme: Tryptophan tryptophylquinone as the redox prosthetic group in methylamine dehydrogenase. *Science 252*, 817–824.

4. Davidson, V. L. (2007) Protein-derived cofactors. Expanding the scope of post-translational modifications. *Biochemistry 46*, 5283–5292.
5. Wang, Y., Li, X., Jones, L. H., Pearson, A. R., Wilmot, C. M., and Davidson, V. L. (2005) MauG-dependent *in vitro* biosynthesis of tryptophan tryptophylquinone in methylamine dehydrogenase. *J. Am. Chem. Soc. 127*, 8258–8259.
6. Wang, Y., Graichen, M. E., Liu, A., Pearson, A. R., Wilmot, C. M., and Davidson, V. L. (2003) MauG, a novel diheme protein required for tryptophan tryptophylquinone biogenesis. *Biochemistry 42*, 7318–7325.
7. Fulop, V., Watmouth, N. J., and Ferguson, S. J. (2001) Structure and enzymology of two bacterial diheme enzymes: Cytochrome cd1 nitrite reductase and cytochrome *c* peroxidase. *Adv. Inorg. Chem. 51*, 163–204.
8. Pettigrew, G. W., Echalier, A., and Pauleta, S. R. (2006) Structure and mechanism in the bacterial dihaem cytochrome *c* peroxidases. *J. Inorg. Biochem. 100*, 551–567.
9. Li, X., Jones, L. H., Pearson, A. R., Wilmot, C. M., and Davidson, V. L. (2006) Mechanistic possibilities in MauG-dependent tryptophan tryptophylquinone biosynthesis. *Biochemistry 45*, 13276–13283.
10. Li, X., Feng, M., Wang, Y., Tachikawa, H., and Davidson, V. L. (2006) Evidence for redox cooperativity between *c*-type hemes of MauG which is likely coupled to oxygen activation during tryptophan tryptophylquinone biosynthesis. *Biochemistry 45*, 821–828.
11. van der Palen, C. J., Slotboom, D. J., Jongejan, L., Reijnders, W. N., Harms, N., Duine, J. A., and van Spanning, R. J. (1995) Mutational analysis of mau genes involved in methylamine metabolism in *Paracoccus denitrificans*. *Eur. J. Biochem. 230*, 860–871.
12. Pearson, A. R., De La Mora-Rey, T., Graichen, M. E., Wang, Y., Jones, L. H., Marimanikkupam, S., Agger, S. A., Grimsrud, P. A., Davidson, V. L., and Wilmot, C. M. (2004) Further insights into quinone cofactor biogenesis: Probing the role of *mauG* in methylamine dehydrogenase tryptophan tryptophylquinone formation. *Biochemistry 43*, 5494–5502.
13. Pearson, A. R., Marimanikkuppam, S., Li, X., Davidson, V. L., and Wilmot, C. M. (2006) Isotope labeling studies reveal the order of oxygen incorporation into the tryptophan tryptophylquinone cofactor of methylamine dehydrogenase. *J. Am. Chem. Soc. 128*, 12416–12417.
14. Li, X., Fu, R., Lee, S., Krebs, C., Davidson, V. L., and Liu, A. (2008) A catalytic di-heme *bis*-Fe(IV) intermediate, alternative to an Fe(IV)═O porphyrin radical. *Proc. Natl. Acad. Sci. U.S.A. 105*, 8597–8600.
15. Jensen, L. M., Sanishvili, R., Davidson, V. L., and Wilmot, C. M. (2010) In crystallo posttranslational modification within a MauG/pre-methylamine dehydrogenase complex. *Science 327*, 1392–1394.
16. Davidson, V. L., Brooks, H. B., Graichen, M. E., Jones, L. H., and Hyun, Y. L. (1995) Detection of intermediates in tryptophan tryptophylquinone enzymes. *Methods Enzymol. 258*, 176–190.
17. Lee, S., Shin, S., Li, X., and Davidson, V. (2009) Kinetic mechanism for the initial steps in MauG-dependent tryptophan tryptophylquinone biosynthesis. *Biochemistry 48*, 2442–2447.
18. Davidson, V. L. (1990) Methylamine dehydrogenases from methylotrophic bacteria. *Methods Enzymol. 188*, 241–246.
19. Husain, M., Davidson, V. L., Gray, K. A., and Knaff, D. B. (1987) Redox properties of the quinoprotein methylamine dehydrogenase from *Paracoccus denitrificans*. *Biochemistry 26*, 4139–4143.
20. Kurnikov, I. V. (2000) HARLEM, University of Pittsburgh, Pittsburgh, PA.
21. Page, C. C., Moser, C. C., Chen, X., and Dutton, P. L. (1999) Natural engineering principles of electron tunnelling in biological oxidation-reduction. *Nature 402*, 47–52.
22. Marcus, R. A., and Sutin, N. (1985) Electron transfers in chemistry and biology. *Biochim. Biophys. Acta 811*, 265–322.
23. Timoteo, C. G., Tavares, P., Goodhew, C. F., Duarte, L. C., Jumel, K., Girio, F. M., Harding, S., Pettigrew, G. W., and Moura, I. (2003) Ca^{2+} and the bacterial peroxidases: The cytochrome *c* peroxidase from *Pseudomonas stutzeri*. *J. Biol. Inorg. Chem. 8*, 29–37.
24. Meunier, B., de Visser, S. P., and Shaik, S. (2004) Mechanism of oxidation reactions catalyzed by cytochrome p450 enzymes. *Chem. Rev. 104*, 3947–3980.
25. Sono, M., Roach, M. P., Coulter, E. D., and Dawson, J. H. (1996) Heme-containing oxygenases. *Chem. Rev. 96*, 2841–2888.
26. Brooks, H. B., and Davidson, V. L. (1994) Free energy dependence of the electron transfer reaction between methylamine dehydrogenase and amicyanin. *J. Am. Chem. Soc. 116*, 11201–11202.
27. Li, X., Fu, R., Liu, A., and Davidson, V. L. (2008) Kinetic and physical evidence that the diheme enzyme MauG tightly binds to a biosynthetic precursor of methylamine dehydrogenase with incompletely formed tryptophan tryptophylquinone. *Biochemistry 47*, 2908–2912.
28. Husain, M., and Davidson, V. L. (1985) An inducible periplasmic blue copper protein from *Paracoccus denitrificans*. Purification, properties, and physiological role. *J. Biol. Chem. 260*, 14626–14629.
29. Giese, B., Graber, M., and Cordes, M. (2008) Electron transfer in peptides and proteins. *Curr. Opin. Chem. Biol. 12*, 755–759.
30. Stubbe, J., Nocera, D. G., Yee, C. S., and Chang, M. C. (2003) Radical initiation in the class I ribonucleotide reductase: Long-range proton-coupled electron transfer? *Chem. Rev. 103*, 2167–2201.
31. Aubert, C., Vos, M. H., Mathis, P., Eker, A. P., and Brettel, K. (2000) Intraprotein radical transfer during photoactivation of DNA photolyase. *Nature 405*, 586–590.
32. Brooks, H. B., and Davidson, V. L. (1994) Kinetic and thermodynamic analysis of a physiologic intermolecular electron-transfer reaction between methylamine dehydrogenase and amicyanin. *Biochemistry 33*, 5696–5701.